Available online at www.sciencedirect.com
ScienceDirect
Journal of Sound and Vibration 309 (2008) 246–261
JOURNAL OF SOUND AND VIBRATION
www.elsevier.com/locate/jsvi

Vibration control for plate-like structures using strategic cut-outs

Manfred H. Ulz[a], S. Eren Semercigil[b,*]

[a]*Institute for Strength of Materials, Technical University Graz, Kopernikusgasse 24, 8010 Graz, Austria*
[b]*Victoria University, School of Architecture Civil and Mechanical Engineering, Footscray Campus, P.O. Box 14428, MCMC, Melbourne, Victoria 8001, Australia*

Received 9 January 2006; received in revised form 17 April 2007; accepted 30 June 2007
Available online 4 October 2007

Abstract

Cut-outs are widely used in plates and shells to facilitate heat dissipation, and to provide access to different components. Because of the presence of the cut-outs, it is expected that the dynamic behavior will deteriorate, and vibration magnitudes will be exaggerated as compared to those of the case without a cut-out. Summary of an investigation is presented in this paper to explore the possibility of making a rectangular cut-out in a plate for the purposes of employing this cut-out as a dynamic vibration absorber.

The process involves numerical modeling using standard finite elements. The numerical predictions are presented in the form of design charts to indicate the conditions under which vibration control may be possible. Then, two variations are presented for comparison purposes, namely a lumped-parameter tuned vibration absorber and an auxiliary flap, instead of an integral cut-out. Finally, simple experiments are described to test the validity of the numerical predictions.

1. Introduction

Plate and shell structures with cut-outs are commonly used in engineering. Ventilation openings to facilitate heat dissipation and openings to provide access are generally the reasons for the presence of these perforations. Cut-outs may also be used to meet the demands for reduced weight of large panels.

It is widely believed that because of the presence of cut-outs, the structure will weaken dynamically and experience an amplification in its response due to an external excitation. The aim of this investigation is to explore the use of cut-outs to improve the dynamic behavior of a plate. Cut-outs are designed in a particular way so that they create flaps within the structure which can vibrate independently. If designed properly, these vibratory flaps should act like a dynamic vibration absorber [1]. For such a design, interaction between remainder of the structure and the vibratory flap should result in a reduction of vibration amplitudes of the structure.

*Corresponding author. Tel.: +61 3 9919 4009; fax: +61 3 9919 4139.
E-mail address: Eren.Semercigil@vu.edu.au (S.E. Semercigil).

0022-460X/$ - see front matter © 2007 Published by Elsevier Ltd.
doi:10.1016/j.jsv.2007.06.068

The intention is to design for transient and random loads which may excite multiple modes. Contribution from multiple modes requires the location of the controller to be compromise, different than designing for a harmonic excitation which would require placing the controller where a peak modal response is expected. This compromise location needs to be determined, along with the tuning frequency, for best effectiveness.

Work has been reported with circular saw blades, where the influence of slots is investigated on the lateral vibration modes [2]. No attempt is reported on the benefits of different designs. The vibration characteristics of plates with cut-outs have been widely investigated [3–6]. In these references, the natural frequencies are calculated in various ways and the influence of the cut-outs is considered. No work is reported on the possible advantages in the dynamic behavior because of the presence of the incisions. An investigation of annular disks with added or removed material [7] gives insight into the related mathematical treatment. However, again no design options for vibration control are carried out. Hence, it is the authors' firm belief that this reported work is the first contribution in the literature.

The presented work is largely based on numerical predictions using standard procedures of finite elements. The next section discusses the suggested vibration control in the form of cut-outs incorporated into a plate-like structure. Two additional configurations are also investigated. The first is a lump-parameter spring–mass absorber. The second is an auxiliary flap in the shape of the suggested cut-outs. The rationale for including the spring–mass absorber is to enable comparisons with an idealized configuration. The auxiliary flap cases, on the other hand, are presented as an alternative to cut-outs, extending the same principals for cases where making incisions may not be practical. Finally, simple laboratory tests are presented with a prototype design to test the validity of the numerical predictions.

2. Numerical model

The chosen plate geometry is rectangular, 2.5 m in length, 1 m in width and 0.002 m in thickness. All edges are clamped. The material properties are those of steel (modulus of elasticity $= 2.1e11\,N/m^2$, Poisson's ratio $= 0.3$, mass density $= 7800\,kg/m^3$). No structural damping is used in the finite elements model which is created using ANSYS [8]. In ANSYS environment, SHELL 63 is selected as the element type. The field is meshed automatically which resulted in an average of 2000 elements. A view of the numerical model is shown in Fig. 1.

The choice of including no structural damping is intentional at this stage. The present objective is to determine the conditions under which a strong interaction (tuning) is established between the flap and the remainder of the plate to be controlled. Including damping is meaningful only after establishing the tuning condition, to dissipate the harmful energy is transferred to the flap as a result of strong interaction.

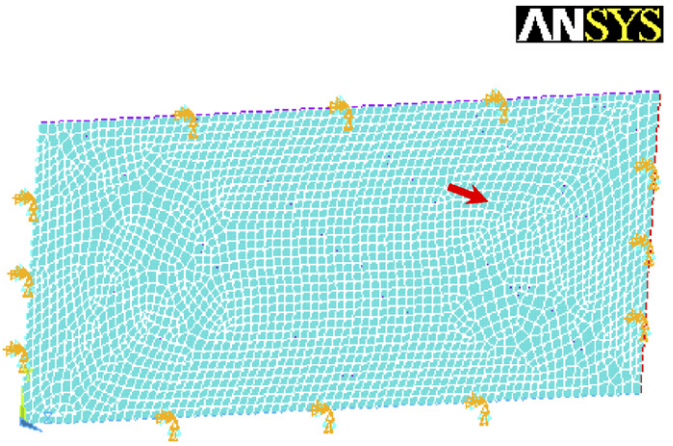

Fig. 1. Model of original plate in ANSYS and location of force—isometric view.

An impact force which is used as the excitation is indicated with an arrow in Fig. 1. The force is located at $x = 1.675$ m (67% of length) and $y = 0.710$ m (71% of width) with a magnitude of 100 N in normal direction. The force is placed away from the symmetry lines to avoid the nodal lines of higher modes.

The first three mode shapes and the corresponding natural frequencies of the plate are given in Fig. 2, for reference. These are obtained from the solution of the eigenvalue problem of the finite elements model, and found to be in close agreement with those in Ref. [9]. In Fig. 2, different shading indicates opposite phase in a particular mode.

Three different aspect ratios of the cut-outs are investigated, namely one square flap (aspect ratio of 1 to 1) and two rectangular flaps (aspect ratios of 1 to 1.5, and 1 to 2.5). In Fig. 3, a schematic drawing is given to indicate the variables used in the simulations. Always the longer side of the absorber is nominated as "a" as shown in Fig. 3. Three locations, where the flap is attached to the remainder of the plate, are examined. First, the absorber is located at 25% of the length "l" of the plate in x-direction (at $x = 0.6250$ m). Second, the absorber is located at 37.5% (at $x = 0.9375$ m). And third, at 50% of the length "l" of the plate (at $x = 1.250$ m). The position of the flap in y-direction is always symmetric with respect to the middle line (at $y = 0.5$ m). Finally, four different absorber sizes are used, namely the length "a" in Fig. 3 is either 7.5% (0.1875 m), or 10% (0.2500 m), or 12.5% (0.3125 m), or 15% (0.3750 m) of the total length "l" of the plate. The width "h" of the incisions is 0.0025 m. The result of this selection is 36 different geometries.

For each of the 36 cases, displacement histories are obtained at 25 locations over the plate for a 0.5 s duration. Numbering of these locations are shown in Fig. 4 for one particular case (where the aspect ratio of the flap is 1 to 1, flap is located at 25% of the total length, and the dimension "a" is 12.5% of dimension "l", hence the label 1to1_25%_12.5% in the caption of the figure). Points 1–15 are located along the edge of the incision and represent the response of the "damaged" area. The next 9 points, Points 16–24, are located in the mid-field, on a grid of equally spaced 3 rows and 3 columns. Point 25 is where the impact force is placed. It should be noted that Points 1–15 move with the different placement of the incision, whereas Points 16–25 are fixed in their position. In some cases, two points may share the same location, such as Points 23 and 9 in Fig. 4.

The equally spaced nine grid points, Points 16–24, represent the general change in dynamic behavior of the plate. These 9 points will be further divided into three regions, later in the next section. Point 13 is of significance since it (along with Points 7 and 8) represents the response of the tip of the absorber. A key

Fig. 2. First three mode shapes and natural frequencies of the rectangular plate with clamped boundaries.

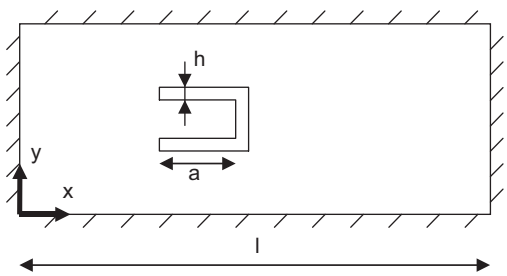

Fig. 3. Design variables for different cases.

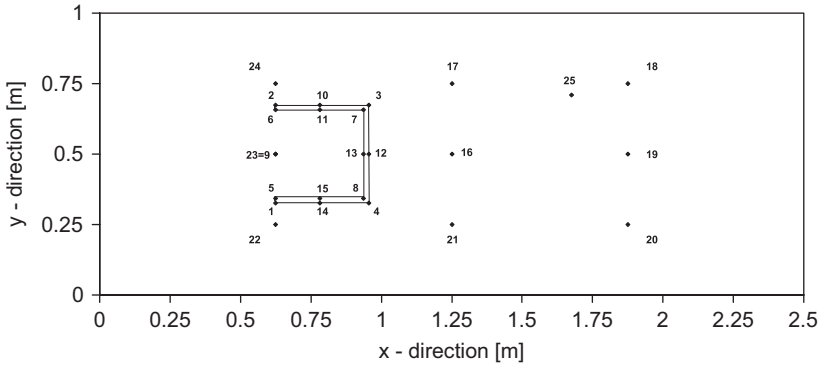

Fig. 4. Numbering of points for case *1to1_25%_12.5%*.

Table 1
Relevant parameters of the square absorber where f_{Plate} is 11.819 Hz

a/l (%)	a (m)	f_{Abs} (Hz)	$f_{\text{Abs}}/f_{\text{Plate}}$
7.5	0.1875	49.645	4.20
10.0	0.2500	27.925	2.36
12.5	0.3125	17.872	1.51
15.0	0.3750	12.411	1.05

indicator of the effectiveness is at Point 9, where (along with Points 5 and 6) the absorber cut-out is attached to the remainder of the plate.

Root mean square (rms) average of displacement is chosen to be indicative of performance. The displacement history of each of the 25 locations is observed, and its rms is calculated to obtain one indicative number. The rms value of each particular point of the plate with an incision, is then divided by the rms displacement of the same location of the original plate. Hence, the rms ratio is now the indicator for the effectiveness of the cut-out. If the ratio is larger than one, an amplification of the response is the result. If the ratio is smaller than one, the incision produces an attenuation. Despite of being an indicator of overall effectiveness, presence of occasional high peaks are masked by rms averaging.

3. Numerical predictions

The objective of the proposed design is for cut-out flaps to act like a dynamic vibration absorber. Conventionally, a dynamic vibration absorber is tuned at the targeted critical frequency of the system, $f_{\text{Absorber}}/f_{\text{System}} = 1$, where "$f$" indicates frequency. However, in this particular case, cut-outs are not independent from the plate. Hence, defining a simple frequency ratio with f_{System} is not meaningful in a strict sense. Nevertheless, the ratio of the fundamental natural frequency of the absorber flap, f_{Abs}, to the fundamental natural frequency, f_{Plate}, of the uncut plate is given in Table 1, for identification purposes. The absorber frequency corresponds to the case where it is cantilevered at its edge where it is normally attached on the remainder of the plate. Again, frequency ratio $f_{\text{Abs}}/f_{\text{Plate}}$ is only an identifier but not as clear an indicator as it would have been for a simple lumped parameter system.

Numerical studies show the cases with a square absorber have the best potential. Hence, discussion will be limited to this particular case, for brevity. Fig. 5 has the rms ratios of 12 cases with the square cut-outs. The horizontal axis indicates the locations of the observed points, whereas the vertical axis has the ratios. The ordinate is arbitrarily cut-off at an rms ratio of 1.5, to clearly show the reduction at an appropriate large scale (in some cases rms ratios become as large as 3). Each row of Fig. 5 represents one size of the absorber, from

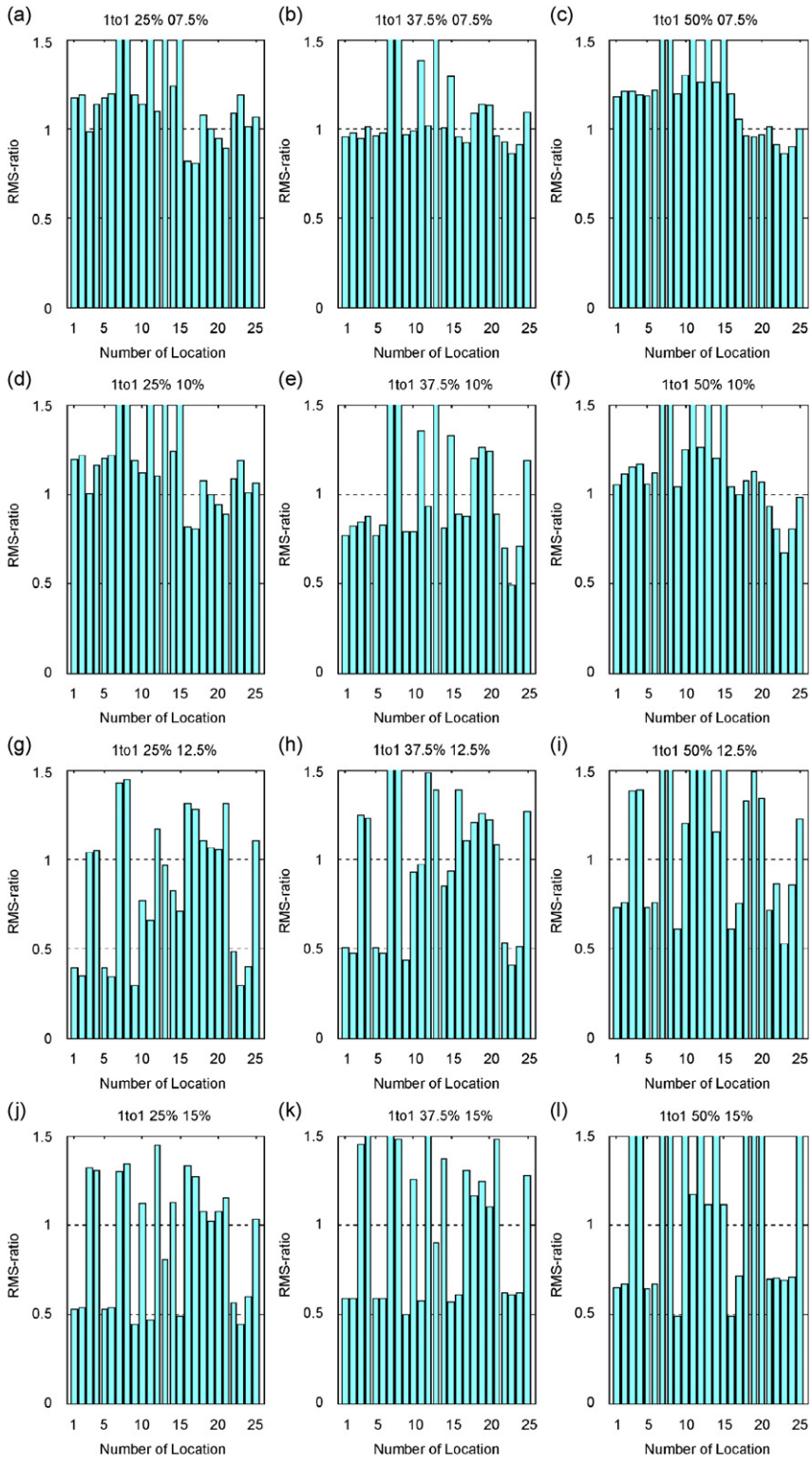

Fig. 5. Variation of rms ratio at different locations for a square absorber. Frequency ratios are: (a)–(c) 4.20; (d)–(f) 2.36; (g)–(i) 1.51; and (j)–(l) 1.05.

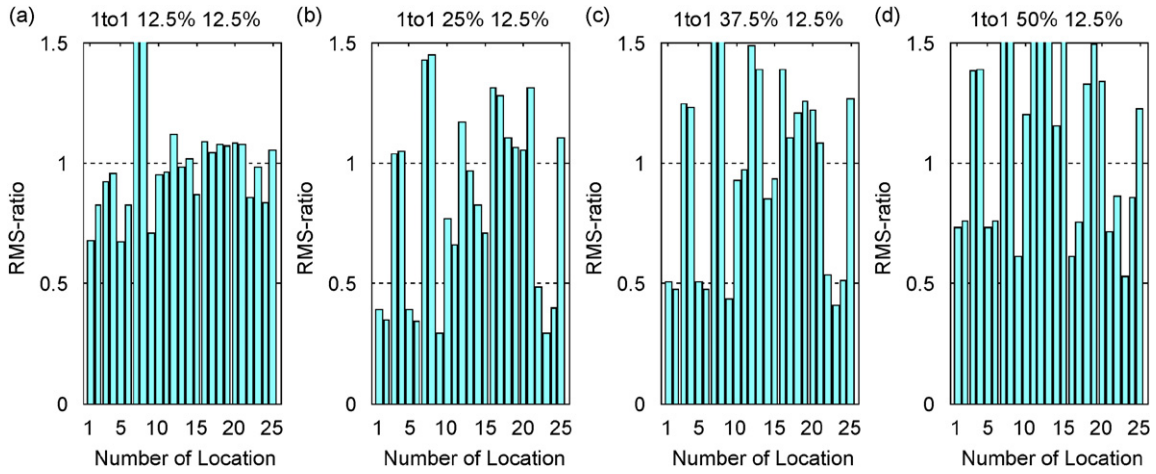

Fig. 6. Variation of rms ratio for a/l of 12.5% and when the absorber is placed at (a) 12.5%, (b) 25%, (c) 37.5% and (d) 50% of the length of the plate.

"a/l" of 0.075–0.15 in descending order. In each row, moving left to right corresponds placing the same size absorber at 25%, at 37.5% and at 50% of the total length of the plate.

Generally, cases with smaller absorbers (7.5% and 10%, in the top two rows), which have frequency ratios of 4.20 and 2.36 (Table 1), seem to be quite ineffective as compared to the cases with larger absorbers (12.5% and 15%, in the last two rows). Therefore, a frequency ratio closer to 1 seems to be more favorable, as expected.

In the third row, cases with an absorber size (a/l) of 12.5% (frequency ratio of about 1.5) are the most promising ones. In this row, rms ratios become smaller at particular locations (and especially at Point 9), as the absorber is placed closer to the left boundary. To check the validity of this observation, the existing cases with a/l of 12.5% are supplemented by one new case, where the same absorber size is placed at the 12.5% of the length of the plate from the left boundary. Fig. 6 shows this new case in frame (a). The remainder three frames are repeated from Figs. 5(g)–(i), for easy reference. For the new case in Fig. 6(a), rms ratios are larger than those in Fig. 6(b), indicating the best performance when the absorber is placed at 25% of the total length from the left boundary.

The reason for 25% length location to be most effective may be speculated by considering the contribution of the second mode to the response of the plate around Point 9. For the uncut plate, the first mode is the in-phase mode with largest deflection in the mid-span. The second mode is the asymmetric mode where the left and right sides move out-of-phase with largest deflections around a quarter of the total length. Placing the absorber at this location seems to produce the best attenuations, whereas moving closer to the fixed wall seems to diminish this effect. Importance of contribution from the second mode is also supported by the somewhat poorer attenuations when the absorber is placed at 50% length, in Fig. 6(d).

As suggested in Fig. 7(a), the plate may be roughly divided into three domains to describe its dynamic behavior with an absorber. First, the section on the left of the absorber attachment experiences a reduction in rms (domain 1, framed dark). The attachment line is the only location where the two sub-structures can interact to exchange information. Hence, the part on the left has the benefit of being directly connected to that exchange gate. Second, the section on the right of the absorber attachment experiences an amplification in rms (domain 2, framed dashed). The reduction of stiffness due to the incisions is more significant here than the suppression effect of the absorber. Third, the section on the right side of the plate shows rms ratios around one (domain 3, framed light). This part of the plate is too far away from the absorber to benefit or to lose because of it.

In Fig. 7(b), the best case (given in Figs. 6(b) and 5(g) earlier) is repeated with different domains marked in the corresponding bars. Points 22, 23 (also Point 9) and 24, which are located in the first domain, show large reductions in rms. These reductions are as much as 70%. Points 16, 17 and 21 are located in the

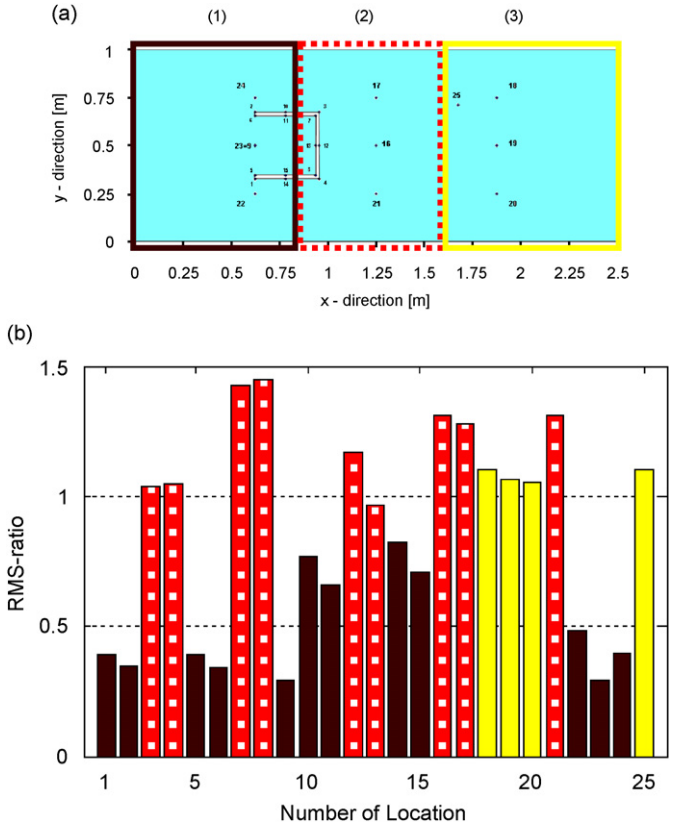

Fig. 7. Showing: (a) the three different domains and (b) corresponding rms ratios for the most effective case of *1to1_25%_12.5%*.

second domain and show amplifications of up to 30%. Points 18–20, in the third domain, are rather unaffected.

For the best case, displacement histories of Points 9 (——) and 13 (……) are shown in Figs. 8(a) and 9(a) for the plate without and with the cut-out, respectively. Figs. 8(b) and 9(b) correspond to the fast Fourier transformations [10]. For the analogy to a classical tuned vibration absorber, Point 9 would represent the structure to be controlled by Point 13.

In Fig. 8(a), displacements of both points are mostly in phase with each other and by comparable magnitudes. In Fig. 9(a), on the other hand, the displacement magnitudes of Point 9 are significantly smaller, while maintaining about the same magnitudes at Point 13 as compared to those in Fig. 8(a). One significant difference in Fig. 9(a) is that the displacement of Point 13 is mostly out-of-phase with that of Point 9. It may be argued that attenuations observed at Point 9 are the consequence of this phase opposition. This observation may also be confirmed with the Fourier spectra given in Fig. 9(b) where the first three spectral peaks of Point 13 correspond to significantly smaller peaks of Point 9. Here, the inherent deficiency, as a result of a 0.5-s total observation time, should be recognized in the frequency resolution.

4. Plate with the lumped-parameter spring–mass absorber

Since the objective of designing a cut-out is to create a flap which behaves as a dynamic vibration absorber, it may now be of interest to replace the flap with a lump-parameter absorber for comparison. Here, the same plate geometry is used for modeling. The absorber is attached at Point 9.

The two critical parameters of an undamped vibration absorber are the mass ratio and the tuning frequency. Mass ratio refers to the ratio of the absorber's mass to the structure's mass. A 10% mass ratio is chosen quite

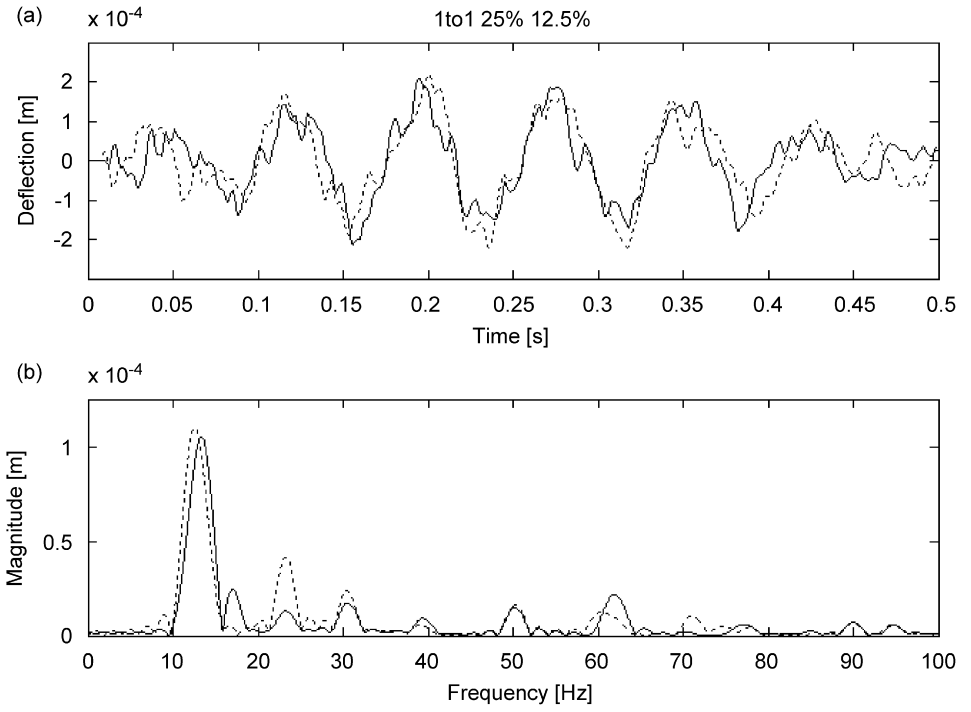

Fig. 8. Displacement (a) history and (b) Fourier spectrum of Point 9 (——) and Point 13 (……) of the uncut original plate.

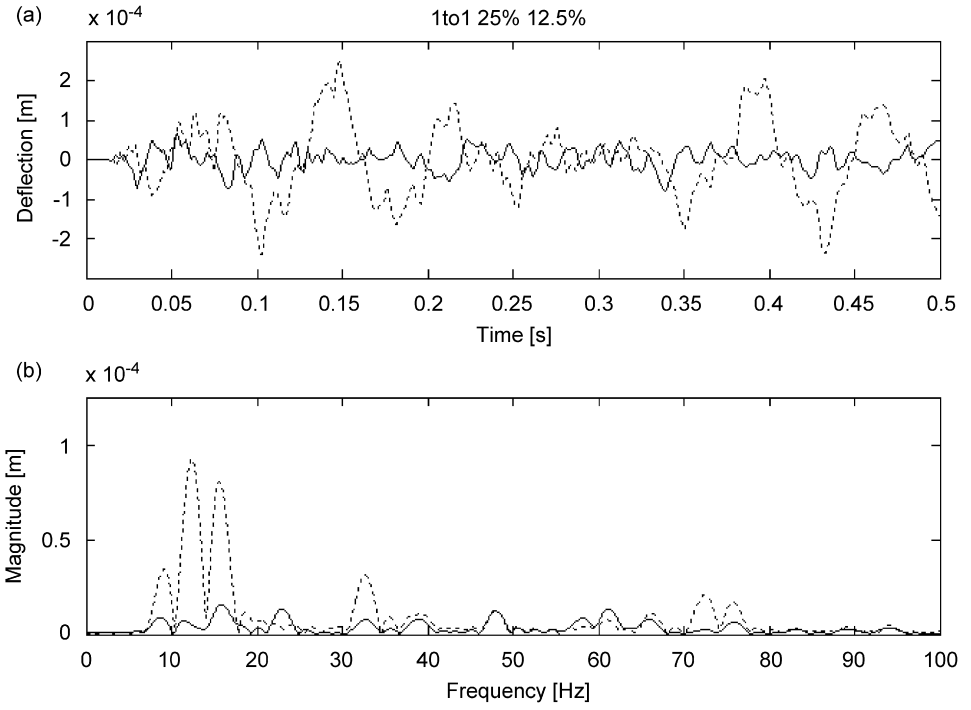

Fig. 9. Same as in Fig. 8 but with the square cut-out placed at 25% of the length from the left boundary and a/l of 12.5% (*1to1_25%_12.5%*).

arbitrarily since no meaningful mass ratio is available for the cut-out cases. The mass of the original plate is 39 kg. Hence, the mass of the absorber is literally taken to be 3.9 kg. It should be noted here that these values represent an effective mass ratio quite larger than 10% in dynamic sense, since only a fraction of the total mass of the plate contributes to its dynamic mass.

The tuning frequency ratio of an absorber refers to the relative values of the natural frequency of the absorber to a critical frequency (usually the fundamental frequency) of the structure. Two frequency ratios of 1.0 and 1.5 are chosen in the light of the predictions reported in the preceding section. Relevant design parameters are given in Table 2.

The rms ratios of the frequency ratio of 1.0 are given in Fig. 10, whereas Fig. 11 corresponds to the frequency ratio of 1.5. Due to the absence of incisions, Points 1–15 are not available. Only the points located on the plate (Points 16–25) are observed in the numerical calculation. Point 9 is also scrutinized which represents the attachment location of the spring.

Same as before, locations which are close to the attachment point of the absorber, benefit more from the absorber, than locations which are further away. Not all points experience a reduction in their rms. The rms ratios for the frequency ratio 1.5 show more effective attenuations than those of the frequency ratio of 1.0. Attachment at 25% of the total length of the plate is again the most promising location.

The displacement histories of Point 9 (——) on the plate and the mass of the absorber (……) are given in Fig. 12(a). Fig. 12(b) corresponds to the fast Fourier transformation of the histories in Fig. 12(a). Response of the original plate is the same as in Fig. 8.

In Fig. 12(a), displacement histories of the attachment point (Point 9) and the tip of the absorber are given. When compared with the histories of the original plate in Fig. 8(a), attenuations may be observed in the displacement of both points. These attenuations are in the order of 70% for Point 9, as suggested in Fig. 11. Hence, when compared to the performance of the cut-out given in Fig. 9(a), a comparable performance is

Table 2
Relevant parameters of the ideal spring–mass absorber

Stiffness (N/m)	Mass (kg)	f_{Abs}/f_{Plate}	f_{Abs} (Hz)
21,508.8	3.9	1	11.819
48,394.7	3.9	1.5	17.729

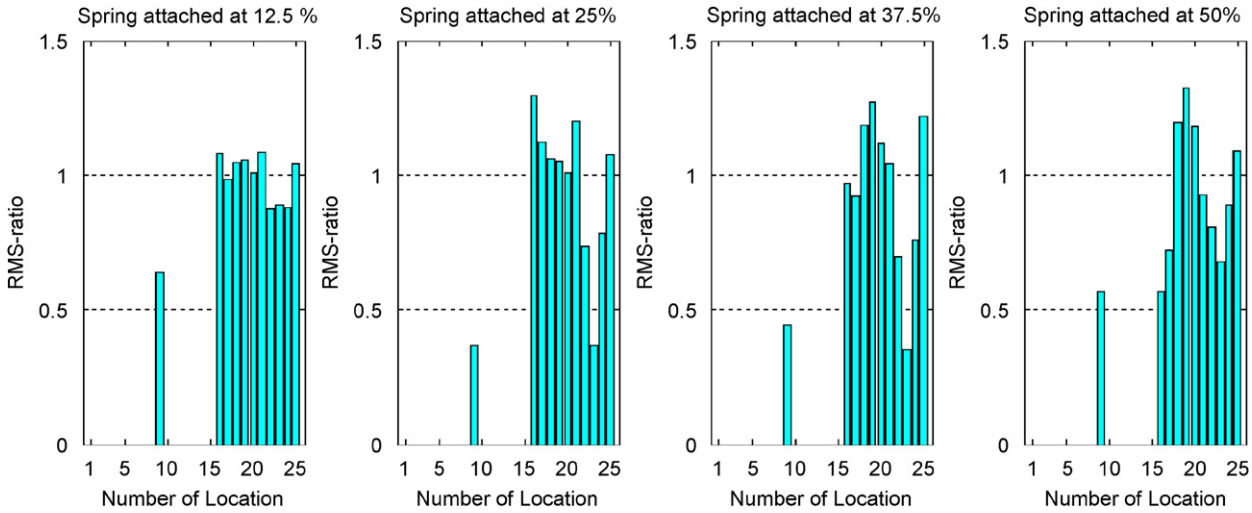

Fig. 10. Variation of rms ratio for the frequency ratio of 1.0 when the spring–mass absorber is placed at (a) 12.5%, (b) 25%, (c) 37.5% and (d) 50% of the length of the plate.

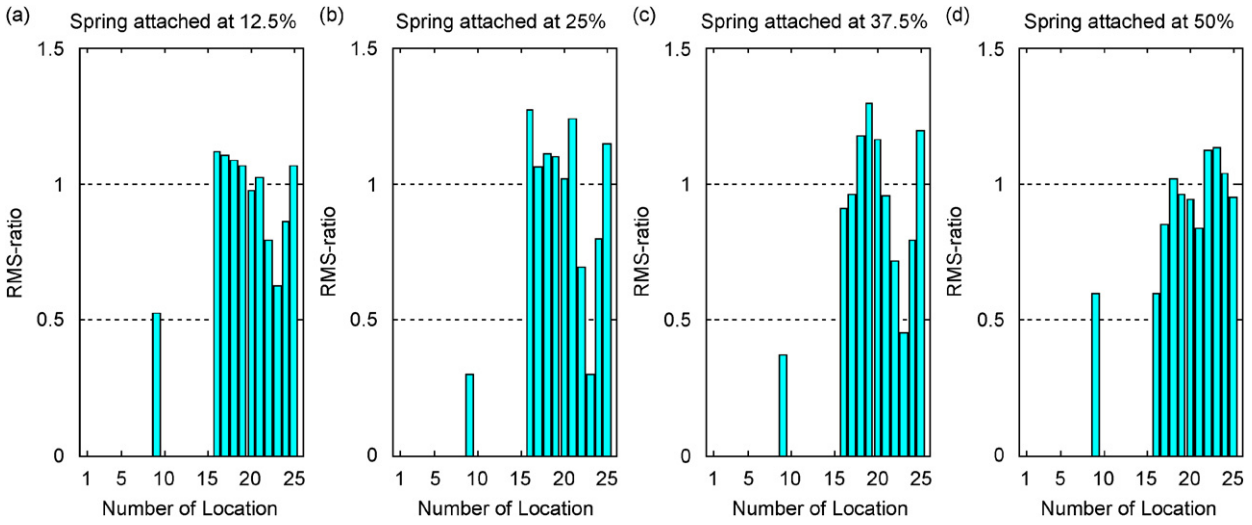

Fig. 11. Same as in Fig. 10 but for the frequency ratio of 1.5.

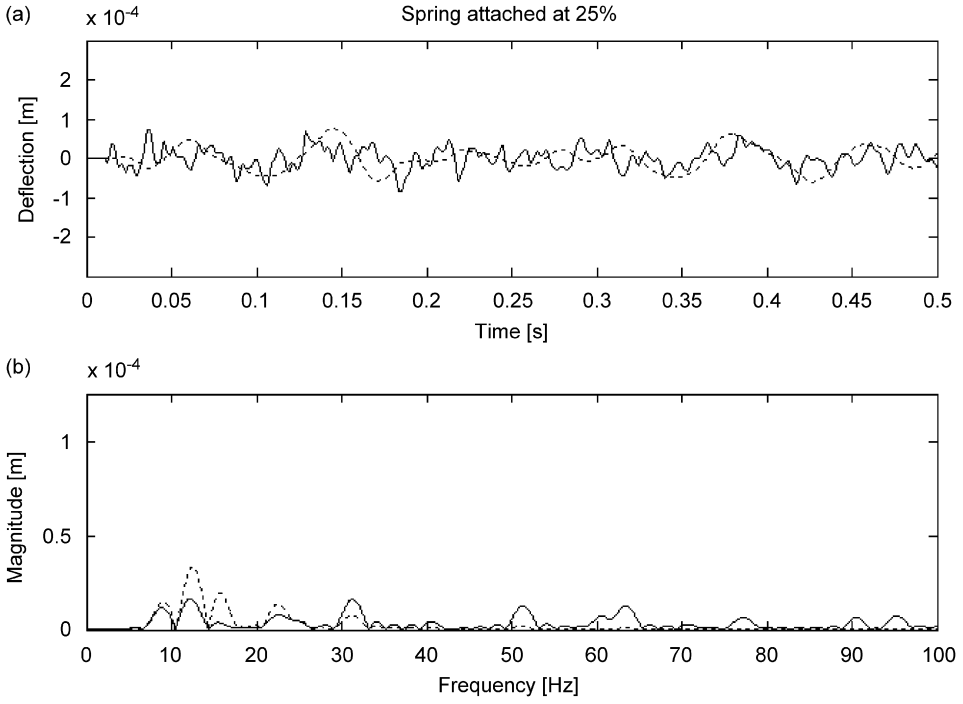

Fig. 12. Same as in Figs. 8 and 9 but with the spring–mass absorber of frequency ratio 1.5.

predicted for the lump-parameter absorber. Displacement of the absorber mass, however, is about half that of Point 13 of the cut-out case. Hence, a cut-out has to work about twice as hard to bring about a comparable control performance. In addition, the frequency content of the lump-parameter absorber is somewhat limited as compared to that of Point 13 in Fig. 9. This is not surprising since the spring of the absorber must act as a low-pass mechanical filter of the many frequencies present in the response of the plate.

In summary, with the lumped spring–mass absorber, pattern of attenuations and amplifications is quite similar to that of the cut-out case. Best attenuations correspond to the same attachment location and the same frequency ratio as the cut-out case. Best attenuations are in the order of 70% at the point of attachment to the plate. Amplifications are quite marginal, about 30% as compared to about 45% with the cut-outs.

5. Plate with an auxiliary flap absorber

Still keeping with the idea of designing a flap which can vibrate independently, and act as a vibration absorber, another variation is presented here. Instead of creating the flap absorber with incisions, it is attached on the plate as an auxiliary structure. Such a design may be more practical where an incision may not be acceptable, but still some means of structural control is desirable. Automotive panels may be considered to be such cases where a flap may be incorporated inside a panel where it would not interfere with other intended design functions, including the esthetic ones.

For comparison, only square flaps with frequency ratios of 1.0 and 1.5 are investigated, similar to those in Section 3. All relevant parameters of design are listed in Table 3. The finite elements model includes the geometry of the flap at a 30° angle from the plane of the plate. This inclination is assumed to be reasonable design decision to avoid contact between the tip of the flap and the plate.

The rms ratios of the 25 locations are presented in Figs. 13 and 14 for frequency ratios of 1.0 and 1.5, respectively. Points 1–15 still correspond to the same locations as in Section 2, even though there is no incision on the plate.

If the response of Point 9 is considered to be critical, frequency ratio of 1.0 produces attenuations of about 65% when the auxiliary flap is attached at 25% of the total length from the left boundary, as suggested in Fig. 13(b). Frequency ratio of 1.5, on the other hand, gives about 55% attenuation at the same location as

Table 3
Relevant parameters of the attached flap

a/l (%)	a (m)	f_{Abs} (Hz)	f_{Abs}/f_{Plate}	m_{Flap} (kg)	m_{Flap}/m_{Plate}
12.5	0.3125	17.872	1.5121	1.52	0.039
15	0.3750	12.411	1.0501	2.20	0.056

m_{Plate} is 39 kg, f_{Plate} is 11.819 Hz.

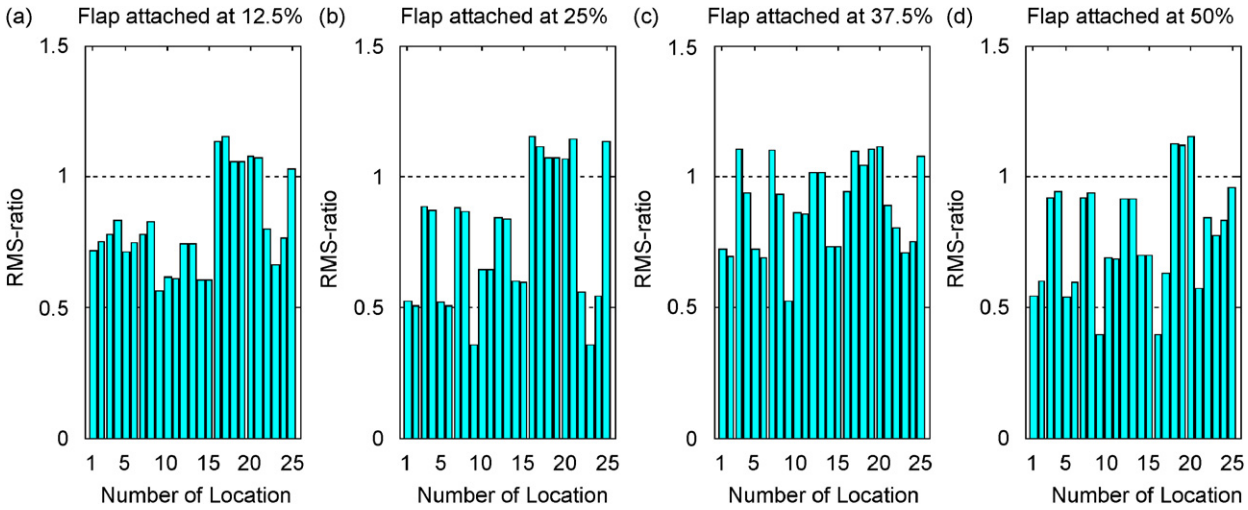

Fig. 13. Variation of rms ratio for a/l of 15% and when the absorber is placed at (a) 12%, (b) 25%, (c) 37.5% and (d) 50% of the length from the left boundary. Frequency ratio is 1.0.

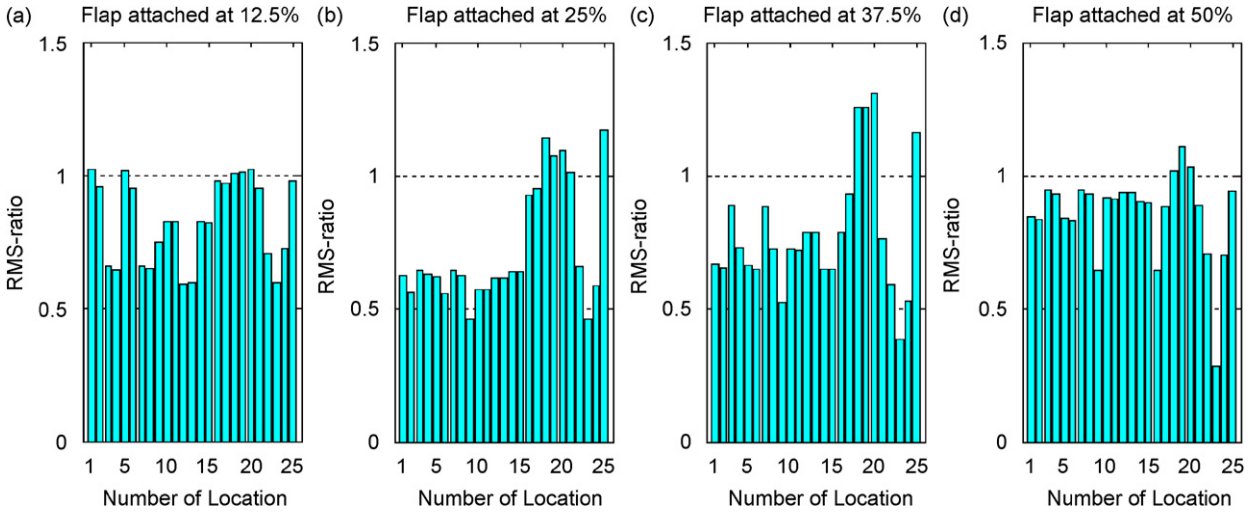

Fig. 14. Same as in Fig. 13 but with flap of size 0.3125 m (12.5% of 2.5 m, frequency ratio of 1.5).

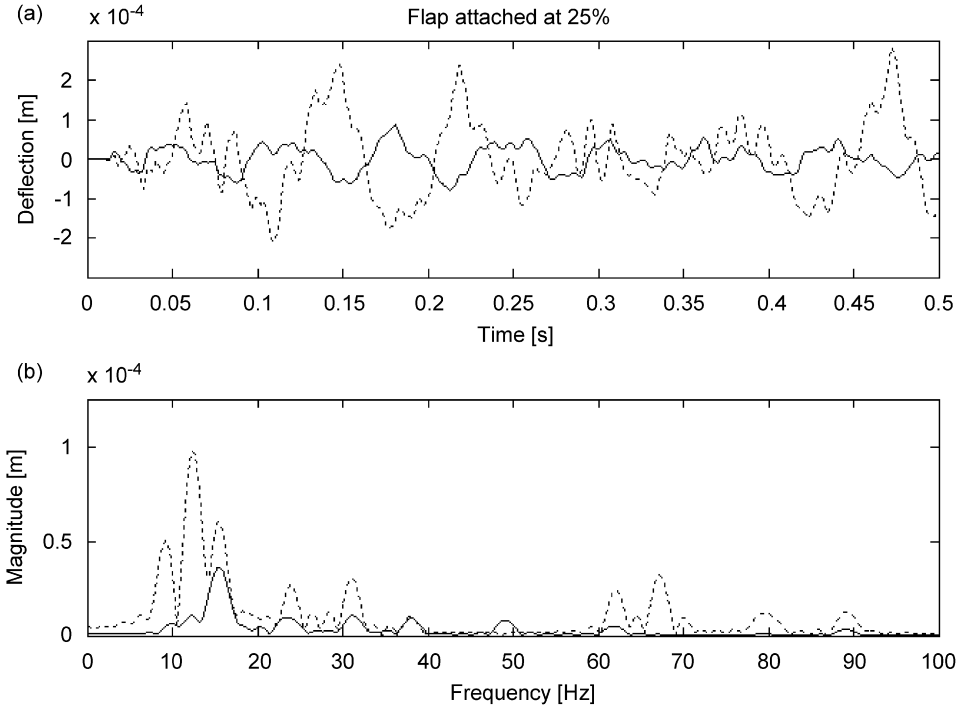

Fig. 15. Same as in Figs. 8, 9 and 12 but with the auxiliary flap of frequency ratio 1.5.

shown in Fig. 14(b). Similar to the case of spring–mass absorber, amplifications are quite marginal as compared to those of the cut-outs. This is particularly true in Fig. 13 where the worst amplification is within 20% of the original plate.

The displacement histories of Point 9 (——), which is the middle of the attachment line, and the tip of the flap (…….) are given in Fig. 15(a). Fourier series representations of these cases are in Fig. 15(b). Again, the corresponding parameters of the original plate are in Figs. 8(a) and (b).

Attenuations of Point 9 are not as effective as those of the cut-out case. In Fig. 15(a), similar to the cut-out case, response of the tip of the flap is mostly out-of-phase with the response of Point 9. Differences may be observed, however, in the frequency spectra where the third spectral peak of the flap, around 17 Hz, has a 40% smaller magnitude than that of the cut-out case. As a result, the largest spectral peak of Point 9 in Fig. 15(b), around 17 Hz, is twice as large as that of the cut-out case in Fig. 9(b).

As a closing observation, there is a curious trend in Fig. 14, for the frequency ratio of 1.5, and for Point 23. Attenuation at this location improve monotonically from frame (a) to frame (d) where the attachment location changes from 15% to 50% of the total length. The best attenuation is about 75%.

6. Experiments

Simple experiments with a laboratory prototype are presented here, to test the validity of the numerical predictions of the preceding sections. The chosen material is medium density fiberboard (MDF). MDF is a type of hardboard made of wood fibers glued under heat and pressure which can be easily drilled and cut. The material properties are found out by simple experiments. The density is obtained to be 895.7 kg/m^3. Measuring the first natural frequency of a cantilever beam made from the same batch of the material gives the Young's modulus to be 6.2706e9 N/m^2. Poisson's ratio v is chosen to 0.3. (Here, no experimental verification is carried out. However, the natural frequencies of the uncut plate change by less than 1.8% after varying v from 0.25 to 0.35. Hence, this small influence is neglected in further investigation.) A structural damping ratio of 1.6% for the first natural mode is obtained with logarithmic decrement.

The original plate is dimensioned 1 m by 0.4 m with all edges fully clamped. The plate is 0.003 m thick. It is framed with timber beams through screws and epoxy glue. The framed plate is then fixed on heavy timber posts as a rigid base to ensure no movement of the frame. Timber posts are leaned against a wall with an angle of 5° from vertical.

The geometry of the plate selected for comparison with the original plate is that which corresponds to the best attenuations with the square cut-out, with a length of 12.5% of the length of the plate, placed at a distance of 25% of the length of the plate from the left boundary (*1to1_25%_12.5%*). Therefore, the square absorber of 0.125 m is positioned at 0.25 m. The width of the incisions is 0.003 m.

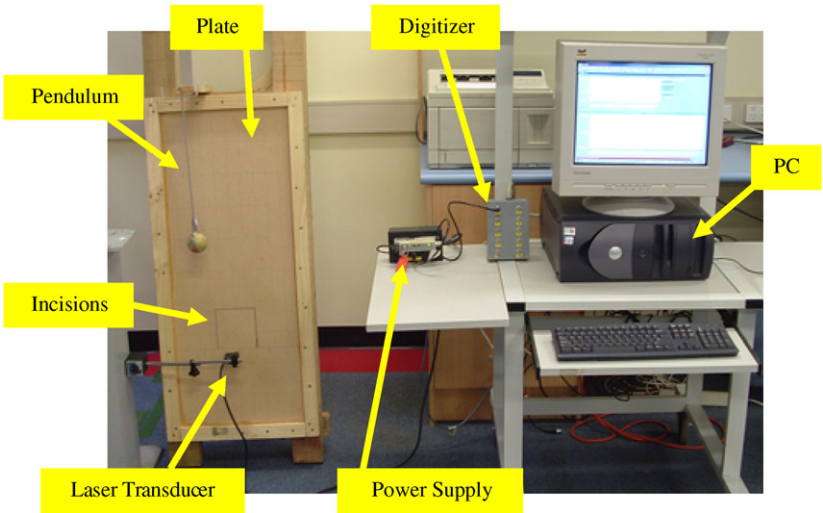

Fig. 16. Laboratory setup (Laser Transducer: Keyence LB-12, semiconductor laser 780 nm, maximum output 3 mW, pulse duration 15 ms, Class III b Laser Product; power supply: Model LB-72, Ser. 107096, Manufactured 910828, Keyence Corporation, 2-13, Aketa-Cho, Takatsuki, Osaka 569, Japan).

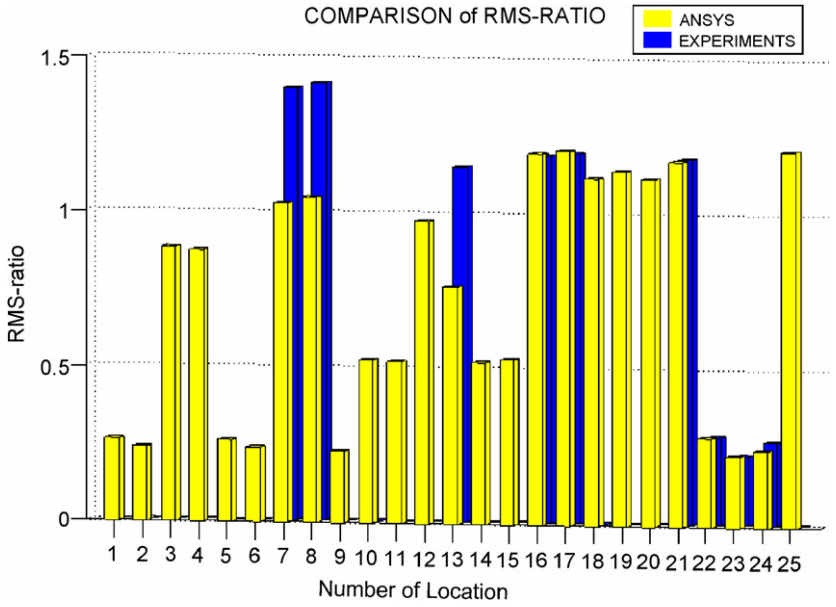

Fig. 17. The rms ratios of numerical predictions (■) and experiments (■) of the MDF plate with the most effective cut-out geometry.

The excitation is a repeatable impulse obtained by striking the plate with the mass of a pendulum released from a pre-determined distance. The plate is struck by the pendulum at the same geometric location as that in the simulations (63% of the length and 71% of the width of the plate).

Fig. 16 shows the laboratory setup. A laser transducer is used to give an analog signal of the displacements of the plate. This analog signal is digitized with a sampling rate of 4000 Hz.

For comparison of the experimental results with predictions from the finite element method, the MDF plate is modeled in ANSYS [8]. The transient excitation is modeled as a pulse of 100 N over 1 ms. These parameters are decided to match the response with the experimental observations of the original plate.

Fig. 17 presents the rms displacement ratios of the predictions and the experiments. Nine locations are observed in the experiments. Points 22, 23 (also Point 9 in this case) and 24 are all located to the left of the absorber. Points 7, 8 and 13 are located at the tip of the absorber. Points 16, 17 and 21 are located in the middle of the plate, to the right of the absorber.

On the left of the absorber, Points 22, 23 (also Point 9) and 24, numerical predictions suggest significant reductions. Here, the agreement of the rms ratios between the experiments and the predictions is very close. Reductions better than 70% are achieved. At the tip of the absorber, predictions suggest surprisingly a reduction in rms at Point 13, and only a small amplification at the corners of the absorber (Points 7 and 8). These predictions could not be verified by the experiments where the rms ratios indicate amplifications of up to 45%. In the middle of the plate, Points 16, 17 and 21, both numerical predictions and experiments show an amplification in rms ratios with a close agreement.

Fig. 18 has the response of the two critical locations, Points 23 (also 9) and 13. The right column has predictions, whereas the left column gives the experimental observations. Odd numbered rows correspond to displacement histories, even numbered rows are the corresponding Fourier series representations.

In general, agreement between the predicted and measured values is quite close. However, there are two crucial differences. First, the first natural frequency of the MDF plate in the experimentations is located at 45.3 Hz instead of the predicted 56.5 Hz. Ideally, all edges of the plate needed to be fully clamped in the experiments. However, this condition is quite impossible to realize practically, causing a difference in the boundary conditions. As a result, the MDF prototype plate is more than 20% off the target frequency. Second crucial difference is at the points located at the tip of the absorber (Points 7, 8 and 13). These points experience

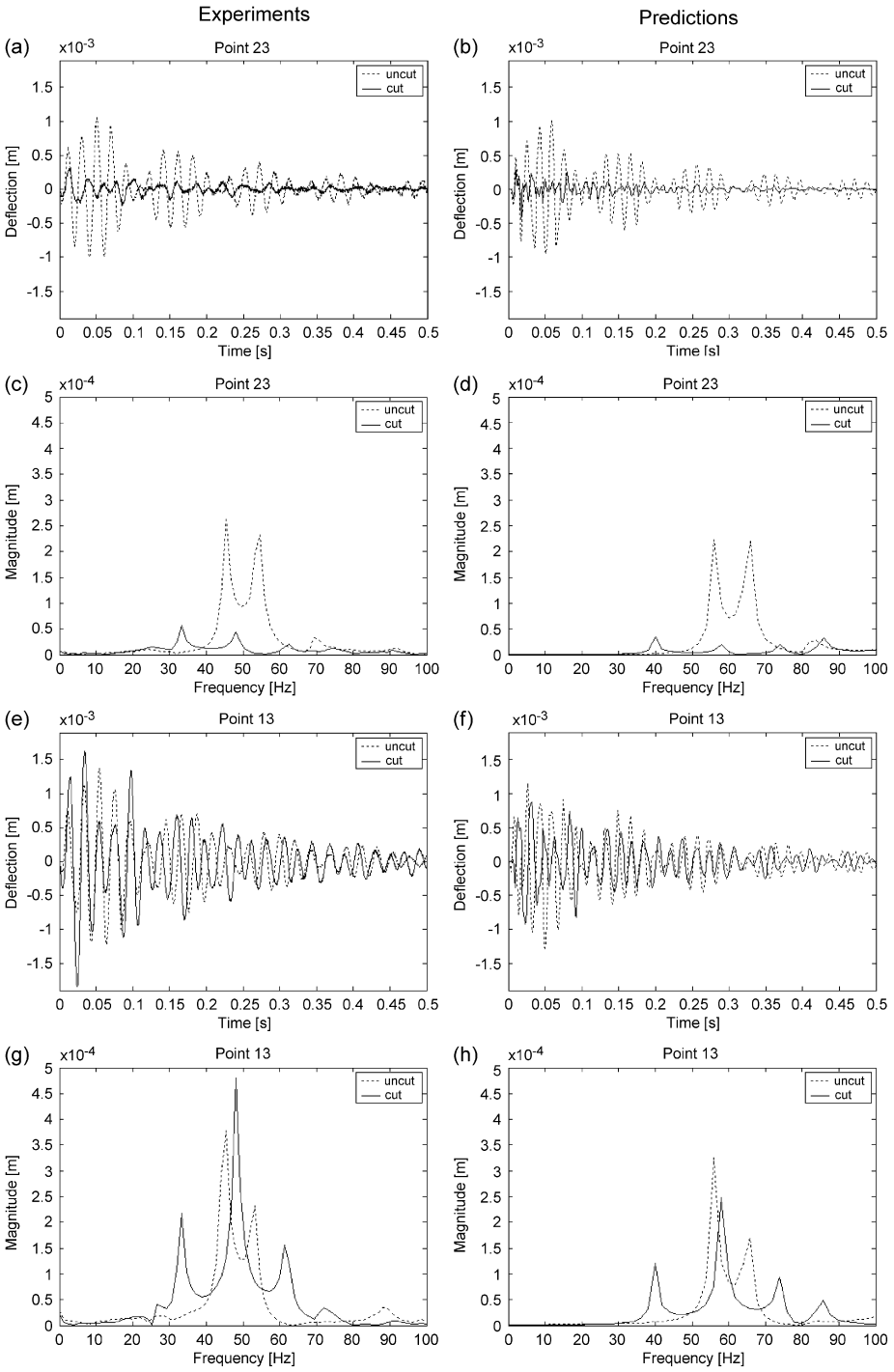

Fig. 18. Displacement histories and Fourier spectra of Point 23 (also Point 9) from (a) and (c) experiments, and (b) and (d) predictions; and of Point 13 from (e) and (g) experiments, and (f) and (h) predictions. Both the original uncut (……) and cut (——) plates are presented.

a larger response in the experiments than in predictions. Limited trials failed to reason this difference. Despite the differences, however, similarities have been found enough to assume the validity of the numerical predictions to a large extent.

7. Conclusions

This work investigates the incorporation of cut-outs into a plate-like structure as a method of vibration control. Cut-outs are intended to create vibratory flaps within the structure and these flaps are intended to act like dynamic vibration absorbers.

- It has been determined that it is not possible to make incisions and obtain attenuations at all points. Locations at the attachment and between the attachment and the left boundary, can experience attenuations of up to 70%. Around the incisions, there is an amplification of response. Away from the incisions, the response is quite similar to that of the uncut plate. Hence, incisions must be placed judiciously according to the location of critical regions of the design.
- A lump parameter spring–mass absorber, produces the same order of attenuations but smaller amplifications as compared to the suggested design. A mass ratio of 10% is used for comparisons.
- An auxiliary flap with the same dimensions of the incisions, produces somewhat poorer attenuations, but smaller amplifications. This design may be preferred if incisions are not necessary for other requirements.
- A dimensional analysis incorporating geometric scaling and material properties is required for a wider applicability of the reported information. Such an investigation should also include the variation of the modal parameters with different cut-outs.
- Finally, all cases reported in this paper relate to a rectangular plate with a large aspect ratio of 2.5. To reveal the effect of the aspect ratio, a square plate has also been investigated, but not presented here for the sake of brevity. A square flap is again found to be effective with a frequency ratio of around 1.0 (rather than 1.5 of the rectangular plate). Best attenuations are in the order of 50% when the incisions are placed at about 25% of the length of the plate from the left boundary [11].

Acknowledgements

We are grateful to Dr. Christian C. Celigoj of Technical University Graz acting as the home supervisor of the first author. Financial support of the Austrian Government and Technical University Graz made this work possible.

References

[1] S.S. Rao, *Mechanical Vibrations*, second ed., Addison-Wesley, New York, 1990.
[2] S. Nishio, E. Marui, Effects of slots on the lateral vibration of a circular saw blade, *International Journal of Machine Tools and Manufacture* 36 (7) (1996) 771–787.
[3] K.M. Liew, S. Kitipornchai, A.Y.T. Leung, C.W. Lim, Analysis of the free vibration of rectangular plates with central cut-outs using the discrete Ritz method, *International Journal of Mechanical Sciences* 45 (2003) 941–959.
[4] J. Yuan, P.G. Young, S.M. Dickinson, Natural frequencies of circular and annular plates with radial or circumferential cracks, *Computers & Structures* 53 (1994) 327–334.
[5] K. Sivakumar, N.G.R. Iyengar, Free vibration of laminated composite plates with cut-out, *Journal of Sound and Vibration* 221 (3) (1999) 443–470.
[6] R.E. Rossi, Transverse vibrations of thin, orthotropic rectangular plates with rectangular cut-outs with fixed boundaries, *Journal of Sound and Vibration* 221 (4) (1996) 733–736.
[7] H. Vinayak, R. Singh, Eigensolutions of annular-like elastic disks with intentionally removed or added material, *Journal of Sound and Vibration* 192 (4) (1996) 741–769.
[8] ANSYS Release 7.0, on-line help.
[9] R.D. Blevins, *Formulas for Natural Frequency and Mode Shape*, Robert E. Krieger Publishing Co., Malabar, FL, 1984.
[10] MATLAB Version 6.1 Release 12.1.
[11] M.H. Ulz, Vibration control of plate-like structures using cut-outs, Technical University, Graz, Dipl.-Arb., 2005.